Plant Soil (2025) 511:1485–1502
https://doi.org/10.1007/s11104-024-07066-y

RESEARCH ARTICLE

Unraveling the dynamics of lignin chemistry on decomposition to understand its contribution to soil organic matter accumulation

Thirunavukkarasu Aswin · Mattias Hedenström · Tobias Sparrman · Mats B. Nilsson · Jürgen Schleucher · Mats Öquist

Received: 8 July 2024 / Accepted: 27 October 2024 / Published online: 19 November 2024

Abstract

Aims Plant inputs are the primary organic carbon source that transforms into soil organic matter (SOM) through microbial processing. One prevailing view is that lignin plays a major role in the accumulation of SOM. This study investigated lignin decomposition using wood from different genotypes of *Populus tremula* as the model substrate. The genotypes naturally varied in lignin content and composition, resulting in high and low lignin substrates.

Methods The wood was inoculated with fresh soil and decomposition was interpreted through mass loss and CO_2 produced during a 12-month lab incubation. Detailed information on the decomposition patterns of lignin was obtained by Two-dimensional Nuclear magnetic resonance (2D NMR) spectroscopy on four occasions during the incubations.

Results The lignin content per se did not affect the overall decomposition and ~60% of the mass was lost in both substrates. In addition, no differences in oxidative enzyme activity could be observed, and the rate of lignin decomposition was similar to that of the carbohydrates. The 2D NMR analysis showed the oxidized syringyl present in the initial samples was the most resistant to degradation among lignin subunits as it followed the order *p*-hydroxybenzoates > syringyl > guaiacyl > oxidized syringyl. Furthermore, the degradability of β–O–4 linkages in the lignin varied depending on the subunit (syringyl or guaiacyl) it is attached to.

Conclusions Our study demonstrates that lignin contains fractions that are easily degradable and can break down alongside carbohydrates. Thus, the initial differences in lignin content per se do not necessarily affect magnitude of SOM accumulation.

Keywords Soil organic matter · Decomposition · Lignin · 2D NMR

Responsible Editor: Michael Luke McCormack.

Supplementary Information The online version contains supplementary material available at https://doi.org/10.1007/s11104-024-07066-y.

A. Thirunavukkarasu (✉) · M. B. Nilsson · M. Öquist (✉)
Department of Forest Ecology and Management, Swedish University of Agricultural Sciences, Umeå SE-90183, Sweden
e-mail: aswin.thirunavukkarasu@slu.se

M. Öquist
e-mail: mats.oquist@slu.se

M. Hedenström · T. Sparrman
Department of Chemistry, Umeå University, Umeå SE-90187, Sweden

J. Schleucher
Department of Medical Biochemistry and Biophysics, Umeå University, Umeå SE-90187, Sweden

Introduction

Soil organic matter (SOM) contains the largest pool of organic carbon in the biosphere second only to

that found in the ocean. Approximately 2400 Gt of organic carbon is estimated to be stored in the top 3 m of soil with about 828 Gt of organic carbon stored in the top 30 cm (Beillouin et al. 2023; Friedlingstein et al. 2020; Lin et al. 2023; Stockmann et al. 2013). Plant biomass is the primary organic input to soils and subsequently transforms into SOM through microbial processing. Besides this, soil physical properties—such as porosity, permeability, and surface area—along with chemical properties, including nutrient availability, pH, cation exchange capacity, and organic matter content, also influence decomposition rates and the soil's capacity for carbon sequestration (Berg and McClaugherty 2020). The current view about SOM is that it is continuous in nature and consists of plant organic fragments of all molecular sizes at various stages of decomposition with a significant contribution from microbial biomass and necromass (Cotrufo et al. 2015; Lehmann and Kleber 2015; Liang et al. 2019). Therefore, understanding the decomposition and transformation of plant inputs is important for long term carbon storage (Prescott 2010; Cotrufo et al. 2015). However, the biogeochemical mechanisms that govern the long-term storage of carbon in soil remain unclear.

Plant biomass is composed of approximately 20–40% lignin, which has been considered challenging to degrade due to its intricate chemical structure (Zhu et al. 2017; Zoghlami and Paës 2019). Lignin in plants forms mainly through the polymerization of three monomers (also known as monolignols) that differ in their degree of methoxylation. After incorporation into lignin, these are referred to as syringyl (S), guaiacyl (G), and *p*-hydroxyphenyl/*p*-hydroxybenzoate (H) respectively (Adler 1977; Boerjan et al. 2003; Vanholme et al. 2010). During the lignification process, the monomers are connected through ether (C–O–C) or carbon-carbon (C–C) linkages. Among them, the most frequent linkage is the β–O–4 linkage while linkages such as β–5, β – β, 5–5, 5–O–4, and β – 1 exist to a lesser extent (Fig. 1) (Ralph et al. 2004; Brown and Chang 2014). To depolymerize such complex lignin structure, microbes use a broad range of extracellular enzymes like peroxidase and phenol oxidase, each employing distinct mechanisms. For instance, phenol oxidase catalyzes non-specific reactions, including the oxidation of Mn^{2+} and Fe^{2+}, which can lead to the depolymerization or transformation of lignin. In contrast, peroxidase can directly oxidize the carbon-carbon (C-C) bonds between lignin monomers, facilitating lignin breakdown through a more targeted approach (Sinsabaugh 2010; Janusz et al. 2017).

The traditional rationale offered for lignin being difficult to decompose is that the microorganisms tend

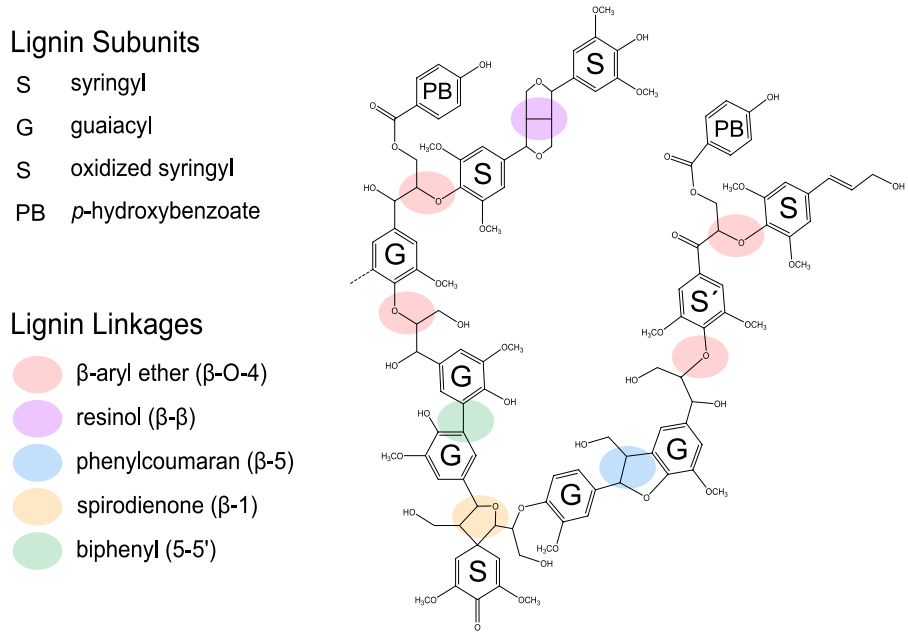

Fig. 1 An example of a lignin polymer. Different possible lignin subunits and lignin linkages are shown. The colors represent different lignin linkages that connect subunits. Note that the structure does not accurately represent the relative abundances of subunits and linkages

to receive a lesser amount of energy in comparison to the energy spent in producing the enzymes for lignin degradation (Schimel and Weintraub 2003; Moorhead and Sinsabaugh 2006; Herman et al. 2008). However, recent studies suggest that lignin degradation is triggered during the early stage of decomposition when the input of an easily decomposable fraction, carbohydrates is abundant. In this way, microbes will have sufficient energy to produce lignin-degrading enzymes (Klotzbücher et al. 2011; Lehmann and Kleber 2015; Angst et al. 2021). Lignin also acts as a binding material within the lignocellulose biomass of plants by being involved in the cross-linking of hemicellulose and cellulose to provide rigidity and stiffness to the cell wall (Boer et al. 2005; Datta et al. 2017). As a result, lignin could physically protect the more labile cell wall polysaccharides from microbial attack or the presence of covalent bonds between lignin and the labile cell wall polysaccharides could potentially protect hemicellulose and cellulose chemically from hydrolysis during the decomposition (Boerjan et al. 2003; Cadisch et al. 1997; Talbot et al. 2012). Thus, lignin could be the important control over the decomposition and transformation of plant inputs. However, the biogeochemical mechanisms by which saprotrophic decay of lignin occurs are still poorly understood.

One major reason for the lack of mechanistic understanding of lignin decomposition is the difficulties in analyzing lignin at adequate resolution. Pyrolysis – Gas Chromatography Mass Spectrometry (Py-GC/MS) is a technique used widely in characterizing different wood types in terms of polysaccharides and lignin-derived products. However, it gives information mainly on lignin derived monomers, leaving out lignin linkages that can vary in their degradation (Lv et al. 2022). Thus, the composition of linkages can be important for decomposition. For instance, syringyl is mostly associated with β-O-4 linkages that are more easily broken by oxidation than the phenylcoumaran (β- 5) and aryl-aryl linkages (5–5') that, in addition to β-O-4 linkages, polymerize guaiacyl (Fig. 1) (Kim and Ralph 2010). Other common methods such as ^{13}C Cross-Polarization Magic-Angle Spinning (CP-MAS) NMR and FTIR-spectroscopy used for OM characterization, lacks in resolution as they can detect only a few broad functional groups (Mao et al. 2017; Ong et al. 2020). However, the two dimensional ^{1}H-^{13}C Heteronuclear Single Quantum Coherence Nuclear magnetic resonance (2D HSQC NMR) is a state–of–art technique that has been increasingly applied in wood and lignin analysis. It has the advantage of analyzing complex organic matrices without extractions or chemical modifications (Kim and Ralph 2014) and results in much higher resolution by allowing for the identification of both lignin subunits and their associated linkages.

The aim of this study is to investigate the degradation of lignin during its initial decomposition stages. To achieve this we conducted a lab incubation experiment using four clones of *Populus tremula* (aspen wood) as model substrates. These clones were chosen as they naturally vary in both lignin content and composition. We hypothesized that the degradation of lignin should be lower than the carbohydrates and the high lignin substrates (HL) will provide more protection to labile plant polymers than in low lignin substrates (LL), thereby reducing the mass loss and carbon respired from the HL substrates. We also hypothesized that differences in lignin composition among the substrates influence its degradation. Therefore, the wood substrates with a higher abundance of syringyl and *p*-hydroxybenzoate units, would decompose faster than substrates relatively higher in guaiacyl.

Materials and methods

Sample properties

Populus tremula clones were used as model substrates for this decomposition study, as it is one of the most common tree species in boreal forests and is naturally rich in genetic variations due to nucleotide polymorphism. This variation significantly impacts the chemical composition of wood (Jalas and Suominen 1989; Escamez et al. 2023). The clones were obtained from the Skogforsk research station in Sävar (63.4°N, Umeå district) and are part of the SwAsp collection, which includes trees from 12 different localities in Sweden (Luquez et al. 2008). Four clones (Clone #: 35, 114, 91, 52) from the SwAsp collection, were chosen for their natural variation in lignin content and composition (Table S2). The wood material was taken from the branches of these clones, with the bark removed completely before further processing. The lignin: carbohydrate ratio was determined

by Py-GC-MS (refer Sect. 2.5). Clones 35 and 114 were categorized as low lignin substrates (LL) with a lignin content of 32 ± 0.6% (mean ± SE) and a carbohydrate content of 67 ± 0.6% (mean ± SE) and clones 91 and 52 were categorized as high lignin substrates (HL), with a lignin content of 41 ± 0.9% (mean ± SE) and a carbohydrate content of 58 ± 0.9% (mean ± SE).

The wood was then cut into small pieces and milled using a Tube mill control (IKA, Germany). The wood was milled to increase surface area, thereby enhancing the availability of sites for enzymatic attack. Although this pretreatment differs from in situ conditions and may affect decomposition rates, our substrate, serves as a conceptual proxy for lignin decomposability on a molecular level, even if it does not fully capture the diversity of lignin morphologies present in natural environments. The milled wood was lyophilized for 72 h and stored at room temperature until the start of the experiment.

Incubation experiment

The soil used in this study originated from the surface O-horizon (0–15 cm) of a boreal spodozol collected from the Kulbäcksliden experimental forest, near Vindeln in the county of Västerbotten, northern Sweden (64°11′N, 19°33′E). Spodzol cover large areas of the northern hemisphere and is thus representative for the boreal forest landscape. The site is a a mixed spruce (*Picea abies*) and pine (*Pinus sylvestris*) stand with *Vaccinium vitis idaea*, *Vaccinium myrtillus*, and *Pleurozium schreberi* as ground vegetation. The soil was transported to the lab and stored at 4 °C overnight after which the soil was homogenized by passing it through a cutting sieve (6×3.5 mm) in its field moist state. During the homogenizing process, needles, cones, visible roots, and other debris were removed. The soil was stored at -20 °C until the start of the experiment.

Organic matter (OM) and carbon (C) contents were determined on replicate subsamples ($n = 4$) of milled wood and homogenized soil. OM was determined by loss on ignition (LOI; 4 h at 550 °C), and organic C was determined using an Elemental Analyzer (Flash EA 2000, Thermo Fisher Scientific, Bremen, Germany). The OM content of the wood was 99.4 ± 0.1% (mean ± SE) with a negligible amount of minerals. The organic carbon and nitrogen contents were 49.7 ± 0.2% and 0.10 ± 0.006% (mean ± SE), respectively, for all wood substrates. For the soil, the OM content was 74.6 ± 0.44% (mean ± SE), with an organic C content of 45.1 ± 0.04% (mean ± SE) (Fig.S1) and organic nitrogen content of 1.38 ± 0.13% (mean ± SE). The soil pH was determined using soil-water suspension method with a soil to water ratio of 1:2, resulted in a pH of 4.5 ± 0.003 (mean ± SE).

The soil incubation experiment was conducted using a respirometer (A. Nordgren Innovations AB, Sweden) to measure CO_2 production hourly. Each incubation jar was equipped with a small vessel containing 10 mL of 0.5 M potassium hydroxide (KOH) and two platinum electrodes. The CO_2 produced during the incubation was trapped in the KOH solution and its production was measured by the induced change in electrical conductivity (Nordgren 1988). For the experiment, 2.55 g dry weight of soil was placed in each 250 mL incubation jar. The moisture content of the homogenized soil was set to -25 kPa, representing optimum moisture content for microbial activity (Ilstedt et al. 2000). Based on the previous litter mass loss studies (Berg et al. 1984; Berg and Ekbohm 1991; Wardle et al. 2003) and in-house incubation studies with boreal forest soils (Nordgren 1988, 1992; Nordgren et al. 1988), approximately 1.5 g dry weight of milled wood in a 160-micron nylon mesh bag (4 cm × 4 cm) was placed inside each jar along with the soil. The size of the nylon mesh bag was chosen to be above 10 µm to ensure unrestricted movement of microbial communities. The samples were incubated in an insulated water bath at 15 °C for 56 weeks, reflecting a typical summer temperature at the site from which the soil was taken. At each of the four sampling time points (12, 24, 36 & 56 weeks after the start of the experiment) 16 sample bags were removed from the incubation jars for analysis, with eight replicates each for both LL and HL substrates. Upon removal, the samples were taken out of the mesh bags and homogenized. Subsamples were then taken for the determination of mass loss (dry weight; 48 h at 80 °C), enzyme activities, and chemical characterization using 2D HSQC NMR and Py-GC/MS.

Enzyme assay

In addition to CO_2 production rates, we used enzyme assays to evaluate differences in the microbial

activity between HL and LL substrates. Specifically, we tracked oxidative enzymes phenol oxidase and peroxidase that are known to be associated with lignin oxidation and broadly reflecting microbial activity. Oxidative enzyme activity was estimated using the protocol from Bonner et al. (2019) that was modified from Saiya-Cork et al. (2002). Approximately 1 g (wet weight) of the decomposed wood substrate was added into two 15 mL falcon tubes. 4 mL of milli-Q water and 1 mL of 5mM L-DOPA (L-3,4-dihydroxyphenylalanine) were added. To one of the two tubes, 0.2 mL of 0.3% hydrogen peroxide was added. The tubes were manually shaken to homogenize and incubated in the dark at room temperature for 2 h. After incubation, the tubes were centrifuged at 3000 rpm for 2 min and the absorbance of each supernatant sample was determined at 460 nm using a spectrophotometer. The increase in L-DOPA oxidation induced by hydrogen peroxide addition was used to calculate peroxidase activity. The absorbance measured from the tube without the addition of hydrogen peroxide was used to calculate phenol oxidase enzyme activity. A concentration gradient of 180 µl of 5mM L-DOPA with 20 µl $NaNO_2$ and 10 µl of 1 M HCl was incubated overnight and a standard curve was plotted by reading the absorbance at 460 nm.

The measured absorbance was subtracted for blank (without L-DOPA) and negative controls (without wood material) and the concentration (mM) for each measured absorbance was determined from the standard curve. Furthermore, the concentration was multiplied by the assay volume (milli-Q water + L-DOPA + hydrogen peroxide) of 5.2 mL. The enzyme activity was normalized to the dry weight of wood used and incubation time, resulting in nmol $g^{-1}min^{-1}$.

NMR spectroscopy

Two dimensional ^{1}H-^{13} C Heteronuclear Single Quantum Coherence Nuclear magnetic resonance (2D HSQC NMR) was used to determine the changes in the lignin composition over time. This technique enabled the detailed analysis of lignin subunits and their associated linkages. Sample preparation was done according to the protocol described in Soucémarianadin et al. (2017). Briefly, 200 mg of freeze-dried wood material were ground in a 50 mL ZrO_2 jar with ten 10 mm ZrO_2 ball bearings using a Retsch PM100 planetary ball mill (Fritsch, Idar-Oberstein, Germany) for 5 × 10 min at 500 rpm with 10 min breaks. 50 mg of ball-milled wood sample was transferred to the NMR tube and dissolved in 600 µl of deuterated dimethyl sulfoxide (DMSO-d6). The sample was mixed thoroughly and left to stand overnight before NMR analysis.

HSQC correlates ^{1}H atoms with their directly bonded ^{13}C atoms through their one-bond J coupling, so that each C-H group gives rise to a cross peak (Fig. 2) at the respective ^{1}H and ^{13}C chemical shifts (in parts per million, ppm). Spectra were acquired on an 850 MHz Bruker Avance III HD spectrometer equipped with a 5 mm cryoprobe (TCI HCN) and automatic sample changer (SampleXpress), using the hsqcetgpsisp2.2 pulse sequence from the Bruker pulse sequence library. Spectra were collected at room temperature (298 K) using 40 scans. A recycle delay of 1 s was used and 128 points were collected in the indirect dimension. Each 2D experiment was approximately 2 h and the raw data were zero-filled to a 2048 × 1024 spectrum size. Spectral widths of 10 ppm (8504 Hz) and 165 ppm (35274 Hz) were used in the ^{1}H and ^{13}C dimensions respectively. Spectra were manually phase- and baseline-corrected and referenced using the residual DMSO peak at 40.0/2.50 ppm. Data were processed with Topspin 3.2 (Bruker BioSpin Corporation, Billerica, USA).

Identification of lignin moieties

The HSQC spectrum was divided into the following regions: aromatic, di-O-alkyl, O-alkyl, and alkyl. To follow the changes in lignin structure, ten peaks in the 2D HSQC spectra were assigned to different lignin moieties and quantified (Table 1). Assignments were based on previously published data (Kim et al. 2008; Del Río et al. 2012). The peaks related to lignin subunits and linkages were identified and integrated into the aromatic and O-alkyl regions (Fig. 2). In Poplar lignin, *p*-hydroxyphenyl content is very low and not detected. Instead, the *p*-hydroxybenzoate groups are present and it is linked to the γ-position of either S or G units (Smith 1955; Goacher et al. 2021).

The relative abundance of each moiety was determined from the specific grouped sum of cross-peak integrals for each sampling time point. Therefore, the sum of subunits was 100% and the sum of linkages

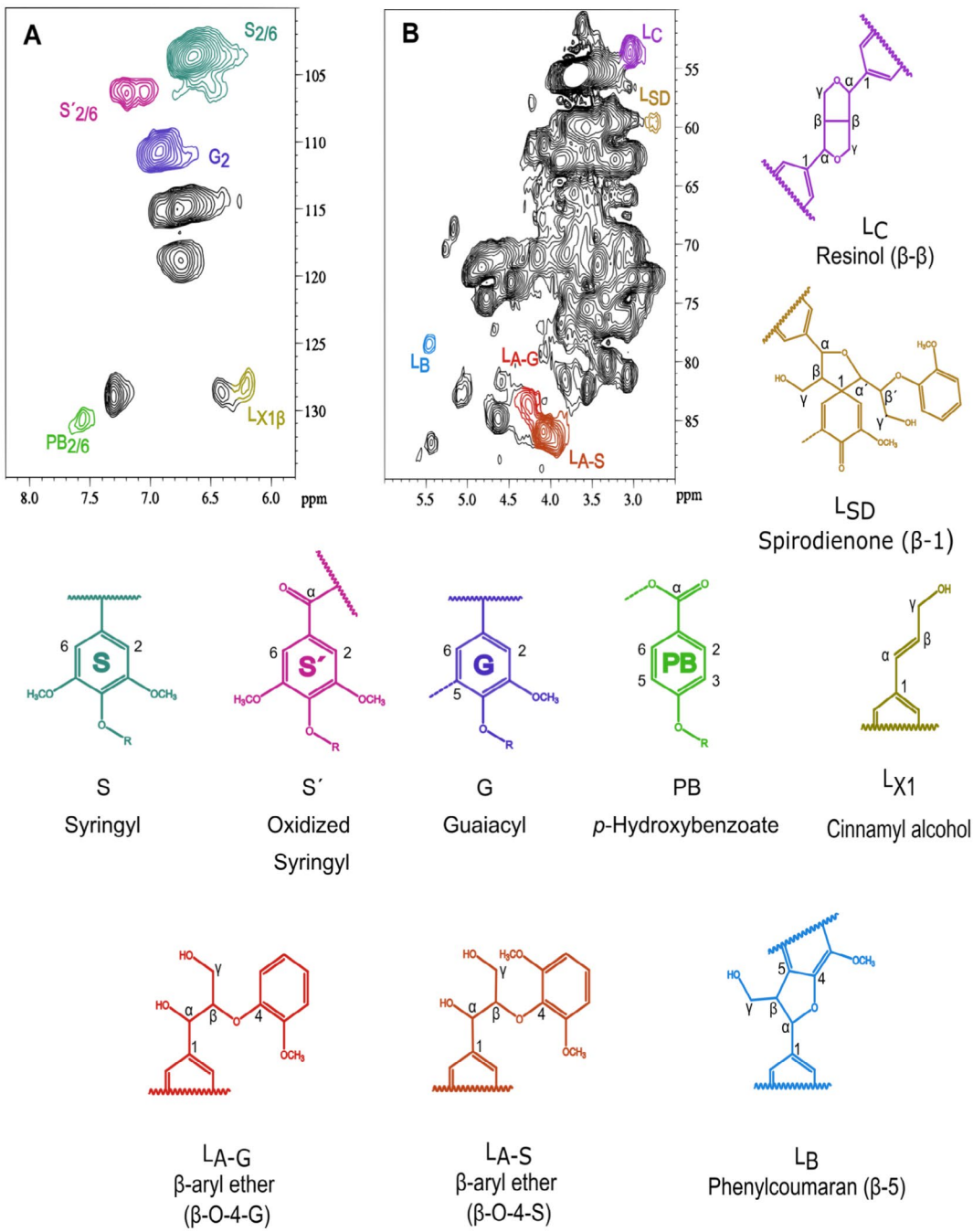

Fig. 2 Peak assignments in the aromatic (**A**) and O-alkyl (**B**) regions of the HSQC spectrum of the undecomposed aspen wood DMSO-extract. Color-coding represents, the chosen lignin linkages and lignin subunit moieties for this study and their corresponding chemical structure shown using respective colors and labeling

Table 1 Assignments of HSQC signals to the lignin linkages and lignin subunit moieties. Each cross peak in the spectrum resulted from the correlation between ^{1}H and ^{13}C, separated by one bond. The ^{1}H and ^{13}C chemical shifts of moieties are shown in parts per million (ppm)

Assignments	δ ^{1}H (ppm)	δ ^{13}C (ppm)
Lignin subunits		
$C_{2,6}$-$H_{2,6}$ in syringyl units	6.65	103.7
$C_{2,6}$-$H_{2,6}$ in C_{α}-oxidized syringyl units	7.19	106.2
C_2-H_2 in guaiacyl units	6.92	110.7
$C_{2,6}$-$H_{2,6}$ in *p*-hydroxybenzoates	7.64	131.2
Lignin linkages		
C_{β}-H_{β} in resinol	3.03	53.5
C_{β}-H_{β} in spirodienone	2.75	59.5
C_{β}-H_{β} in β-O-4' ethers linked to guaiacyl	4.26	83.5
C_{β}-H_{β} in β-O-4' ethers linked to syringyl	4.08	85.8
C_{α}-H_{α} in phenylcoumaran	5.43	86.9
C_{β}-H_{β} in cinnamyl alcohol	6.20	127.9

was 100%. In this way, we see the abundance of these moieties over time. A decreasing trend of the relative abundance of a certain moiety as a function of sampling time meant that it degraded to a larger extent than other moieties included within the same group. Likewise, an increasing trend implies less degradation relative to other moieties within the same group. In cases where several peaks could be used to track the same sub-structure, the best-resolved peak was chosen (Table 1).

Pyrolysis gas-chromatography mass spectrometry (Py-GC/MS)

To determine the differences in the lignin contents of the model substrates, milled wood from the four clones (see above) was analyzed by Py-GC/MS for their lignin: carbohydrate ratios. This was repeated at the end of the experiment to evaluate the extent to which the polymeric groups had decomposed in relation to each other. Approximately 75 µg of freeze-dried sample was transferred to auto sampler containers (Eco-cup SF, Frontier Laboratories, Japan). The Py-GC/MS setup consisted of an oven pyrolyzer with an auto sampler (PY-2020iD and AS-1020E, FrontierLabs, Japan) connected to a GC/MS system (Agilent, 7890 A-5975 C, Agilent Technologies AB, Sweden). The setup of pyrolysis GC/MS conditions was similar to (Gerber et al. 2012). The pyrolyzing temperature was set at 450 °C. The temperatures of the pyrolysis GC interface and GC injector were at 340 °C and 320 °C respectively. Helium was used as the carrier gas with a split ratio of 16:1. The gas saver mode was activated with a flow rate of 3 mL min^{-1} after one minute to vent away the pyrolysate remaining in the pyrolyzer oven. DB-5MS capillary column (30 m × 0.25 mm i.d., 0.25 µm film thickness; J&W, Agilent Technologies AB, Sweden) was used to separate the pyrolysate. The GC temperature was increased from 40 °C to 320 °C with a rate of 10 °C min^{-1}. The GC/MS interface was maintained at 300 °C. The mass spectrometer operated at unit mass resolution with a quadrupole type analyzer and the mass range was scanned from m/z 30 to 500 at 3.1 scan s^{-1}. For ionization, 70 eV electron bombardment was used (Tolu et al. 2015).

From the Agilent Chemstation Data Analysis (Version E.02.00.493), the raw data were exported to NetCDF and proceeded in R (version 2.15.2, 64 bits) similar to the processing method specified in (Jonsson et al. 2005; Tolu et al. 2015). Alternate regression (MCR-AR) is used to process the data that involves chromatogram smoothing and alignment, background correction, and multivariate curve resolution (Karjalainen 1989). Then for each sample, a data table with peak areas and a data text file with mass spectra for each peak were obtained. The latter was imported into the mass spectra library software 'NIST MS Search 2.0' to annotate the peaks based on spectra from the library 'NIST/EPA/NIH 2011'. In total, 55 peaks were annotated, excluding CO_2. The annotated peaks were categorized either carbohydrates or lignin (guaiacyl, syringyl and phenols) (Supplementary Table S1). The relative percentage of carbohydrates and lignin were then determined by normalizing to the total sum of peak areas for each sample.

Statistical analysis

The difference in mass loss between the HL and LL substrates after 56 weeks and the initial difference in the lignin: carbohydrates ratio between HL and LL substrates were determined using the unpaired two-sample t-test. Both the assumptions of normality and homogeneity of variance were satisfied. To

investigate if the difference in lignin abundance of the substrates significantly affected the increase in total accumulated CO_2-C over time and lignin: carbohydrates ratio determined from pyrolysis products, we conducted two way repeated measure Analysis of Variance (ANOVA). The normality assumption of data was satisfied but the variance of the differences between groups was not equal (assumption of sphericity). To solve this, the p-values were adjusted using Greenhouse-Geisser and Huynh-Feldt corrections (Girden 1992). The difference in the enzyme activities for the HL and LL substrates and the difference between the phenol oxidase and peroxidase enzyme activity among substrates were determined using three-way repeated measure ANOVA. The assumption of normality was satisfied and the p-values were adjusted for violation of the assumption of sphericity.

The relative percentage of each molecular moiety was analyzed for the difference in decomposition between the HL and LL substrates by using Linear mixed effects (LME) models. Using the lme4 package in R (Bates et al. 2015), LME models were performed by considering the different starting values of four clones individually as the random factor. *p*-values of the fixed factors (HL & LL substrates) were approximated by F-test using Type II ANOVA tests with Kenward-Roger Degrees of Freedom using the "car" and "lmerTest" packages in R (Kuznetsova et al. 2017; Kenward and Roger 1997). The significance of random effects was tested using the maximum likelihood ratio test (Zuur et al. 2009). If the random effects were not significant then two way repeated measure ANOVA was performed. The post hoc test of pairwise comparison was performed using emmeans packages in R. The *p*-values were adjusted using the Tukey method (Searle et al. 1980). All statistical analysis was performed with R environment software v.4.0.1(R Core Team 2021).

Results

Overall decomposition of model substrates

The overall decomposition rate of our substrates was interpreted through mass loss and the total CO_2-C produced during the incubations. The total CO_2-C generated from the soil in the absence of substrates over 56 weeks was 53 ± 0.7 mg (mean $\pm$ SE). After accounting for this, the decomposition of HL and LL substrates resulted in 466 ± 29 mg and 443 ± 34 mg of CO_2-C, respectively, representing $62 \pm 4\%$ and $59 \pm 4\%$ of carbon lost from the substrates, with no significant difference between them ($p = 0.55$)

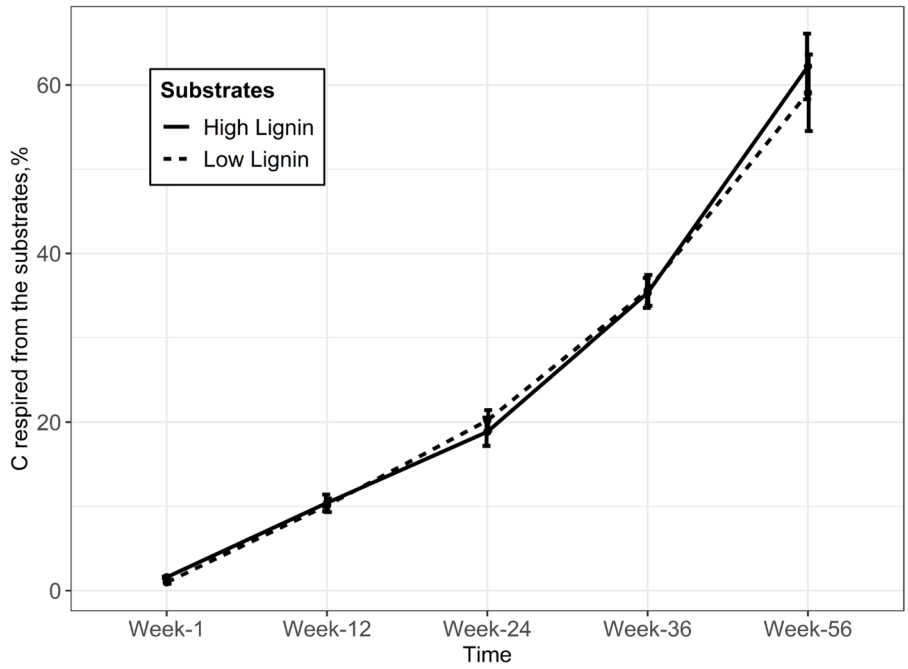

Fig. 3 Average percentage (relative to C content of added substrate, $n = 8$) of carbon respired from high and low lignin substrates as function of incubation time. The error bars represent standard error ($\pm$SE)

(Fig. 3). Similarly, the total mass loss for HL and LL substrates was 59 ± 5% and 50 ± 5%, respectively, also showing no significant difference ($p = 0.23$). Furthermore, carbon loss through mass reduction and CO_2-C respiration remained statistically similar for both the substrates ($p = 0.24$). The enzyme activity did not differ significantly neither between peroxidase and phenol oxidase activity ($p = 0.28$) nor between HL and LL substrates ($p = 0.41$). By the end of week 56, the peroxidase activity for HL and LL substrates was 69 ± 10 nmol g^{-1} min^{-1} (mean ± SE) and 100 ± 10 nmol g^{-1} min^{-1} (mean ± SE) respectively. During the same period, the phenol oxidase activity for HL and LL substrates was 57 ± 14 nmol g^{-1} min^{-1} (mean ± SE) and 77 ± 15 nmol g^{-1} min^{-1} (mean ± SE) respectively (Fig. 4).

The difference in the lignin: carbohydrates ratio (determined by Py-GC/MS) among our substrates at the start of the incubation was statistically significant ($p < 0.001$). The mean lignin: carbohydrates ratio of HL substrates was 0.72 ± 0.02 (mean ± SE) and 0.48 ± 0.02 (mean ± SE) for the LL substrates. By the end of week 56, the mean lignin: carbohydrates ratio of HL substrates was 0.57 ± 0.01 (mean ± SE) and 0.58 ± 0.05 (mean ± SE) for the LL substrates (Fig. 5). The lignin: carbohydrates ratio had a significant interactive effect between substrates and time ($p < 0.05$). Relatively more lignin was decomposed compared to carbohydrates in the HL substrates, while lignin and carbohydrates decomposed at equal rates in the LL substrates (Fig, S2, S3 and S4).

Decomposition of lignin subunits and linkages

The changes in the relative abundance of lignin subunits and lignin linkages across different time points were statistically significant (Figs. 6 and 7; $p < 0.0001$). Within the lignin subunits, the relative abundance of syringyl decreased significantly ($p < 0.0001$ for HL and LL substrates) during the period from 24 −56 weeks (Fig. 6a). However, the relative abundance of oxidized syringyl increased significantly ($p < 0.0001$ for HL and LL substrates) during the weeks 12–36 (Fig. 6d). For the guaiacyl, the relative abundance did not change significantly until the week 36 ($p = 0.07$ for HL and LL substrates) (Fig. 6b).

Within the lignin linkages, the relative abundance of β-O-4 linked to guaiacyl increased significantly ($p < 0.0001$ for HL substrates; $p < 0.001$ for LL substrates) during the weeks 12–56 (Fig. 7b). In contrast, the relative abundance of β-O-4 linked to syringyl did not change significantly ($p = 0.15$ for HL substrates; $p = 0.09$ for LL substrates) during this time

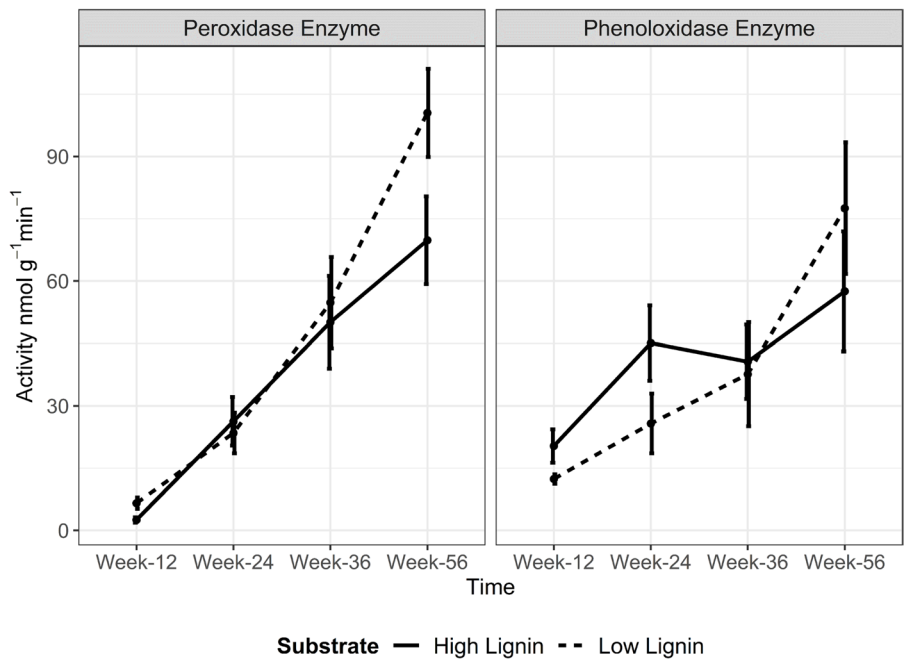

Fig. 4 The average ($n = 8$) peroxidase and phenol oxidase activities for the high and low lignin substrates. The error bars represent standard error (± SE)

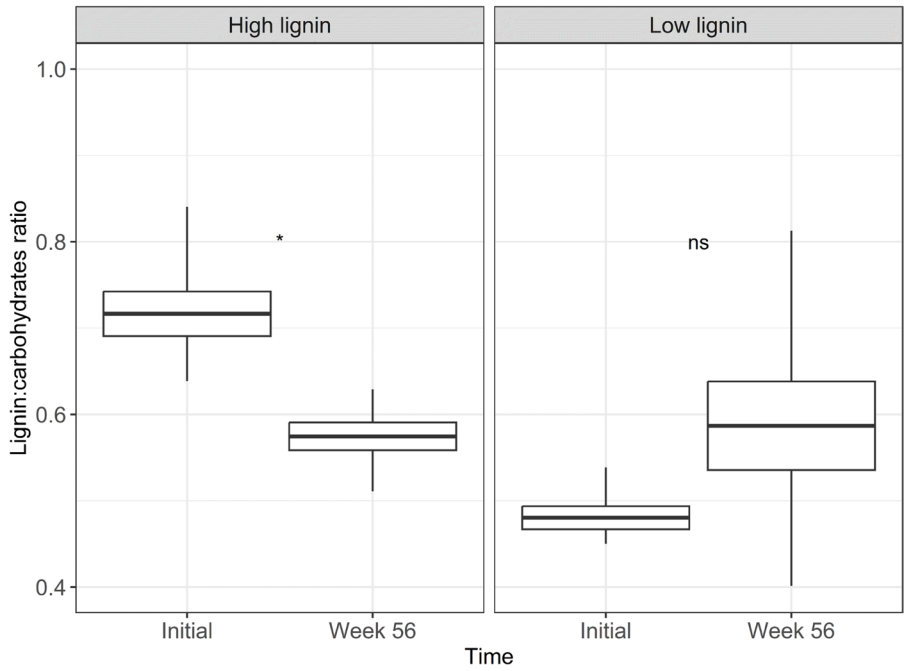

Fig. 5 Lignin: Carbohydrates ratio of pyrolysis products from high and low lignin substrates for the initial, undecomposed, substrates and after week 56 of incubation. The boxplot shows means ($n=8$) and standard errors (±SE). The sign (*) indicates p-value < 0.05 and (ns) indicates statistical non-significance

period (Fig. 7a). For the first 12 weeks, the relative abundance of β-O-4 linked to syringyl increased significantly ($p<0.001$ for HL substrates; $p<0.01$ for LL substrates) (Fig. 7a). During the same time, the relative abundance of resinol linkages decreased significantly ($p<0.01$) for HL substrates but not for LL substrates ($p=0.29$) (Fig. 7c). For the cinnamyl alcohol linkages, the relative abundance decreased significantly for LL substrate ($p<0.05$) but not for HL substrates ($p=0.43$) during the weeks 12–36 (Fig. 7d). In addition, the relative abundance of spirodienone linkages decreased ($p<0.0001$ for HL and LL substrates) significantly during the weeks 12–36 (Fig. 7f). Finally, for the phenylcoumaran linkages, the relative abundance increased significantly until week 56 ($p<0.001$ for HL and LL substrates) (Fig. 7d).

The random intercept LME model was employed to address the initial variations in the relative abundance of lignin linkages and subunits among the substrates. After controlling for the initial randomness, the decomposition patterns of β-O-4 linked to syringyl ($p=0.15$), β-O-4 linked to guaiacyl ($p=0.39$), and phenylcoumaran ($p=0.10$) linkages showed no significant differences between HL and LL substrates (Fig. 7a, b & d). The decomposition patterns of resinol ($p<0.05$) and cinnamyl alcohol linkages ($p<0.05$) were significantly different between HL and LL substrates (Fig. 7c & e) but not for the spirodienone linkages ($p=0.06$) (Fig. 7f). Similarly, for the lignin subunits, there was no significant difference between HL and LL substrates in the decomposition pattern of syringyl ($p=0.09$), guaiacyl ($p=0.39$), *p*-hydroxybenzoate ($p=0.83$), and oxidized syringyl ($p=0.12$) units (Fig. 6). However, there was a significant interaction effect between the substrate type and time on the abundance of syringyl ($p<0.05$) and *p*-hydroxybenzoate ($p<0.05$). The relative abundance of syringyl decreased for HL substrates between weeks 36–56 ($p<0.001$). However, for the LL substrates, the relative abundance of syringyl did not significantly change during the same period (Fig. 6a). In the same way, the relative abundance of *p*-hydroxybenzoate decreased significantly for HL substrates ($p<0.0001$) from initial until week 56, but for the LL substrates, the relative abundance of *p*-hydroxybenzoate did not change significantly ($p=0.77$) during the same period (Fig. 6c).

Discussion

This study investigated lignin degradation during its initial decomposition phase using different high lignin (HL) and low lignin (LL) genotypes aspen wood as a model substrate. Our results suggest that the

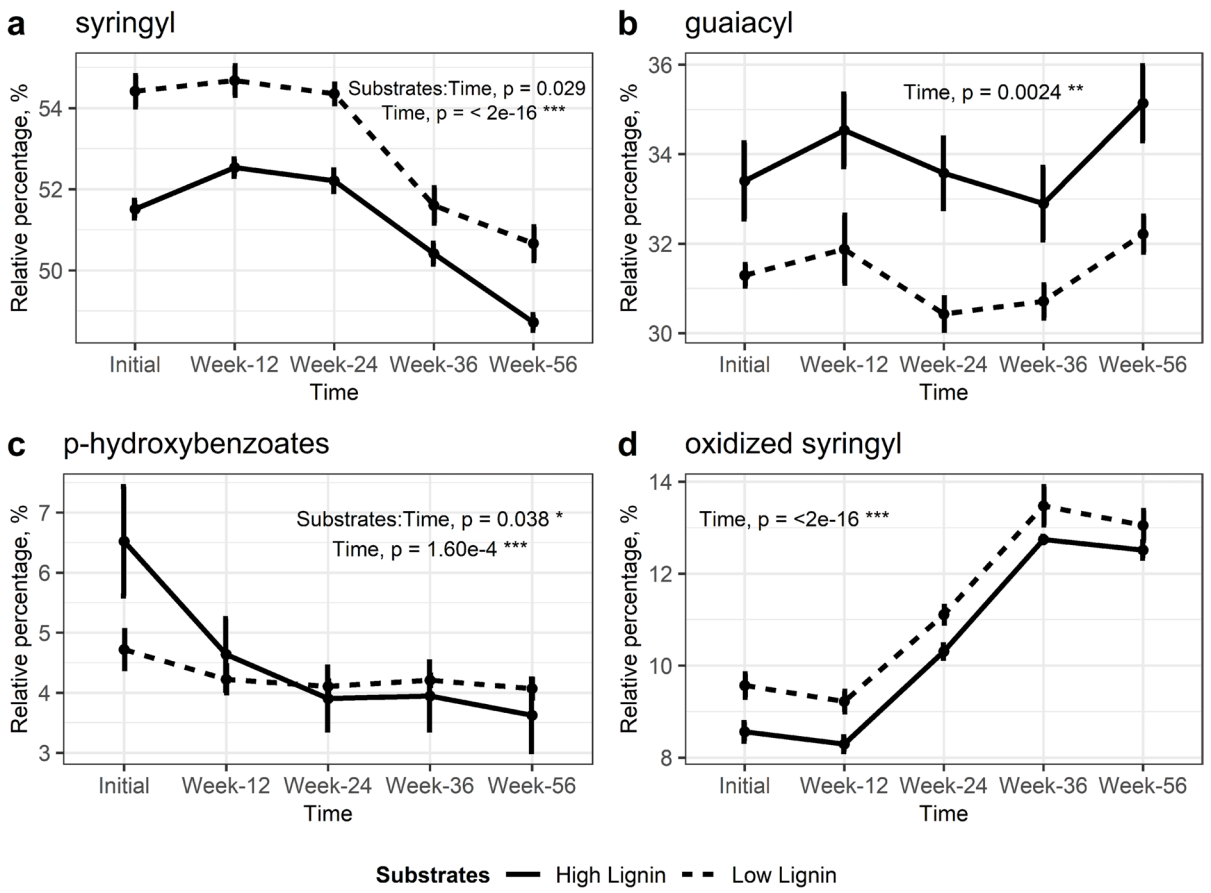

Fig. 6 Temporal dynamics of average ($n = 8$) relative percentage of lignin subunits in the high and low lignin substrates (**a**-**d**). The error bars represent standard error (± SE). The sign (*) indicates statistical significance

difference in lignin content and composition did not impact the decomposition of model substrates as CO_2 production, mass loss, and oxidative enzyme activity between our model substrates were similar (Figs. 3 and 4 & S5). Furthermore, the lignin degraded relatively more than carbohydrates for the HL substrates and was on par with the degradation of carbohydrates for the LL substrates (Fig. 5). This suggests that the potential for lignin degradation during the decomposition is high, Similar results of active degradation of lignin during the early decomposition phase were shown by He et al. (2019) in a 180 days laboratory incubation experiment using leaf litter from two plant species *Fagus lucida* and *Schima parviflora.* In addition, there is an increasing amount of laboratory and field studies suggesting that lignin is not particularly resistant to microbial decomposition during its initial stages of the decomposition (Huang et al. 2023; Kalbitz et al. 2006; Klotzbücher et al. 2011; Miltner and Zech 1998; Yue et al. 2016).

The observation that CO_2 production and mass loss are similar suggests the absence of significant physical constraints induced by the lignin on the microbial access to the cell wall components of e.g. polysaccharides. This is also supported by Talbot et al. (2012) who concluded that physical protection of cell wall polysaccharides by lignin appeared to play a smaller role than the chemical protection of the decay of the plant material. They used litter from *Arabidopsis thaliana* that was genetically modified to differ in guaiacyl content, as compared to the wild type. Litter from the high guaiacyl plant lost polysaccharides at a similar rate as compared to the wild type, which led to their similar decay rates. Likewise, in our study, we observed lignin degradation to be more similar to that of carbohydrates for the model substrates. Thus, we

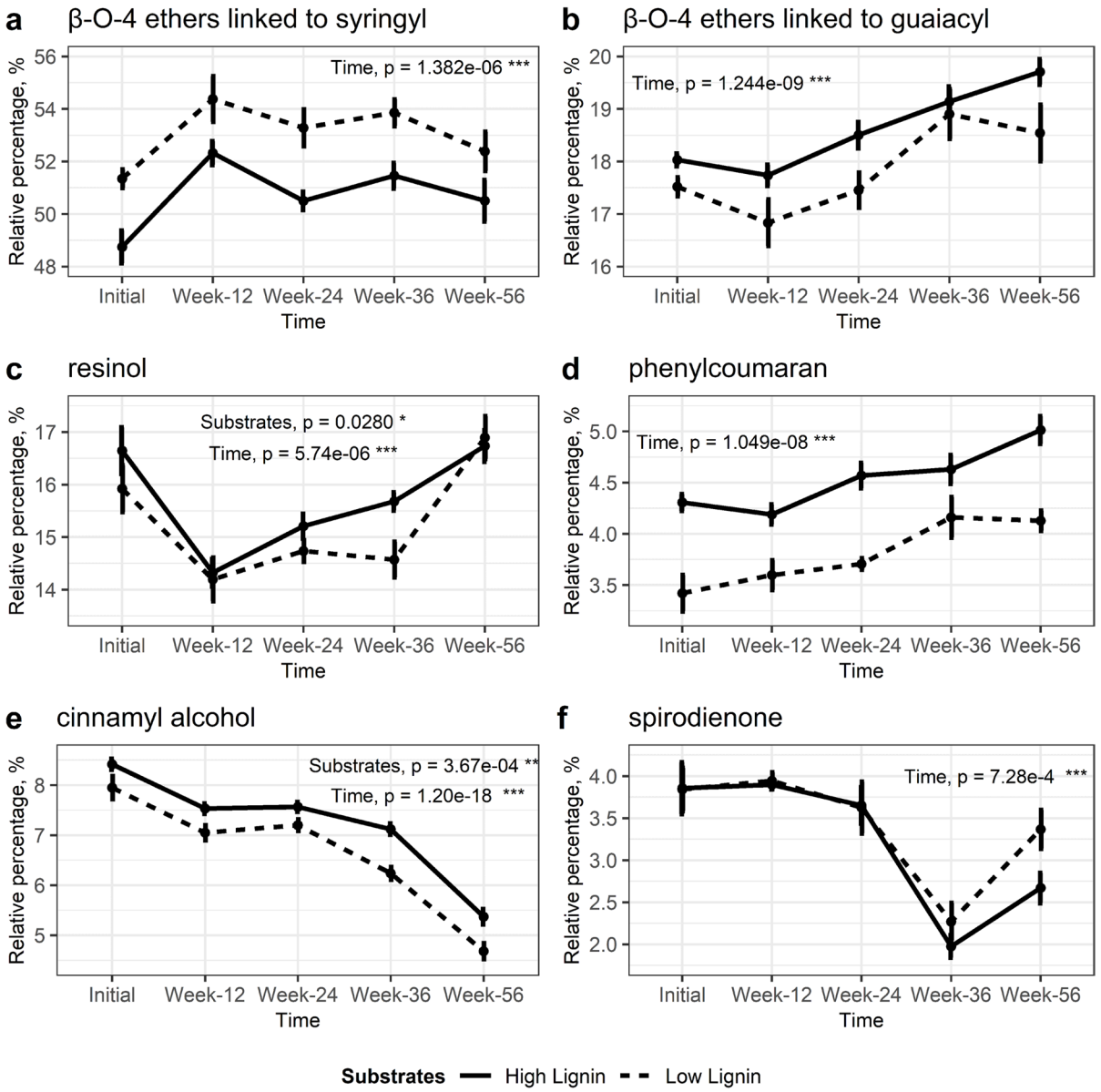

Fig. 7 Temporal dynamics of average ($n = 8$) relative percentage of lignin linkages in the high and low lignin substrates (**a**-**f**). The error bars represent standard error (±SE). The sign (*) indicates statistical significance

can reject our hypothesis that lignin degradation proceeds slower than carbohydrates.

During decomposition, the reduction in the abundance of syringyl was greater than that of guaiacyl (Fig. 6a & b). This is consistent with several studies that have reported a decrease in syringyl relative to guaiacyl during the decomposition of various plant litters (Otto and Simpson 2006; Pisani et al. 2015; Strukelj et al. 2012; Thevenot et al. 2010; vandenEnden et al. 2018). Because the HL substrates contained more lignin initially, we hypothesized HL substrates to retain more lignin during the incubation. This was partially true as the changes in the lignin chemistry over the course of the experiment, between HL and LL substrates were similar except for the *p*-hydroxybenzoate. The relative abundance of *p*-hydroxybenzoate decreased faster in HL substrates compared to LL substrates (Fig. 6c). This implies that

similar to the *p*-hydroxyphenyl (H-lignin) (Campo et al. 2019; Goñi et al. 1993; Otto and Simpson 2006; Soucémarianadin et al. 2017; vandenEnden et al. 2018), *p*-hydroxybenzoate also degrades faster and belong to faster-decomposing lignin fraction, alongside syringyl, as compared to guaiacyl.

Interestingly, a small proportion of syringyl was found to be in its oxidized form (Cα-oxidation) in our model substrates and its fraction increased significantly during decomposition (Fig. 6d). This indicates that oxidized syringyl was more resistant to degradation compared to any of the other lignin sub-units. Studies have shown that Cα-oxidation deactivates the aromatic ring from undergoing electrophilic substitution that determines their subsequent reactions after enzyme oxidation (Kirk et al. 1986; Kawai et al. 2002). Therefore, Cα-oxidation would suppress the degradation of lignin further (Van Erven et al. 2019; Chen et al. 2021). Moreover, microbes depolymerize lignin using various peroxidases and phenol oxidase enzymes that lead to Cα-Cβ cleavage, Cα-oxidation, β-ether cleavage, or aromatic ring cleavage reactions. However, the increase in Cα-oxidation fraction was mainly due to the relative decrease in the abundance of other subunits and there was no clear evidence of additional formation of oxidized syringyl (Cα-oxidation) resulting from the de-polymerization of lignin.

The differences in the degradation of lignin subunits can be attributed to the different stability of various linkages that these units form (Talbot et al. 2012). The β–O–4 linkages are more associated with syringyl than with guaiacyl (Kim and Ralph 2010) and they are considered more easily degradable than other lignin linkages. Moreover, because of the availability of the C5 position for the formation of linkages such as β–5, 5–5, and 5–O–4, guaiacyl was more resistant to degradation (Boerjan et al. 2003). This is in line with our results as we found β–O–4 linked to syringyl linkages decreased in abundance as compared to guaiacyl's phenylcoumaran (β–5) linkages (Fig. 7a & d). In addition, the linkage β–O–4 linked to guaiacyl was more resistant to microbial decomposition than β–O–4 linked to syringyl (Fig. 7a & b). Thus, the degradability of β–O–4 linkages depends on the degradability of the respective subunits to which they are attached. Along with β–O–4 linkages, a decrease in the abundance of other minor linkages such as resinol, cinnamyl alcohol, and spirodienone was also evident in our samples (Fig. 7c, e & f). During the initial phase of decomposition (< 12 weeks), the abundance of resinol (β– β) linkages, which is more resistant than β–O–4 linkages decreased faster compared to that of β–O–4 linked to syringyl linkages (Fig. 7a & c). Thus, our results suggests other unknown factors also regulates lignin linkage stability.

A common challenge in lignin degradation studies is the difficulty in generalizing results, as significant variations often occur among studies (Thevenot et al. 2010; Polman et al. 2021). These variations can be attributed to differences in e.g. the source and type of plant material and soil properties. Different plant species exhibit distinct lignin content and composition, particularly in the subunits that make up lignin and the distribution of linkages between them (Lourenço and Pereira 2018). For instance, in gymnosperms like pine and spruce, lignin is predominantly composed of guaiacyl (G-units), with minor amounts of *p*-hydroxyphenyl (H-units). In contrast, angiosperm dicots have lignin that mainly consists of guaiacyl (G-units) and syringyl (S-units). Softwood tends to have a higher abundance of H-units, with slightly elevated levels also found in grasses (Vanholme et al. 2010). Moreover, different parts of plants, such as internodes, leaves, and roots, exhibit variations in the presence of condensed lignin structures (where lignin units are attached at the C2, C3, C5, or C6 positions of adjacent units) and uncondensed structures (where these connections are absent) (Bertrand et al. 2006; Machinet et al. 2009). Various biotic and abiotic factors further impact lignin polymerization in plants (Moura et al. 2010; Liu et al. 2018; Renström et al. 2024), which in turn can be reflected in the overall rate of lignin degradation.

In our model substrates, the degradation patterns of lignin moieties were consistent between the HL and LL substrates. The composition of our model lignin in terms of S, G, and H-type subunits, is representative of the lignin found in a range of boreal plant species, though the relative distribution of these subunits may vary among species. On a molecular level, this distribution provides an effective conceptual proxy across diverse plant materials, offering a reliable framework for studying lignin degradation. Additionally, under low pH conditions like in our study, lignin can undergo non-enzymatic oxidation by hydroxyl radicals produced via the Fenton reaction, which oxidizes Fe^{2+} to Fe^{3+} (Jung et al. 2009; Shah et al. 2015; Op De Beeck

et al. 2018). It is also possible that other soil types with varying mineral compositions could exhibit different behaviors due to stronger interactions between mineral constituents and organic matter, potentially exerting greater control over decomposition (Cotrufo et al. 2013, 2015; Huang et al. 2019). However, irrespective of the specific degradation mechanisms or the structural variations within lignin, HSQC NMR can be applied to investigate the resistance of different lignin subunits and linkages that determine the lignin degradation rate.

Conclusions

HSQC NMR offers the unique possibility to investigate the degradation of lignin comprehensively, involving not just the various subunits of the lignin polymers but also the different polymerizing linkages. This technique also allows for the identification of sections within the lignin polymer that are more susceptible to enzymatic degradation, distinguishing them from those that contribute significantly to the stability and accumulation of SOM. Our results contradict the more traditional view on lignin degradation as it occurred at rates similar to that of carbohydrates. Instead, it lends support to the recent paradigms of energetically coupled decomposition of lignin and carbohydrates. Our findings emphasize that the type of subunits and their linkages determine lignin stability. Furthermore, our study reveals that lignin contains fractions that are easily degradable and can break down alongside carbohydrates, suggesting that initial differences in lignin content alone do not necessarily contribute to the magnitude of SOM accumulation.

Acknowledgements We thank Kathryn Robertson, Hannele Tuominen, and Stefan Jansson for help in obtaining material from the SwAsp collection; The SLU Stable Isotope Laboratory (SSIL), UPSC/KBC Biopolymer Platform (BAP), and the Swedish NMR Center for help with analysis.

Author contributions Aswin Thirunavukkarasu: Formal analysis, Investigation, Data Curation, Visualization, Writing – original draft, Writing – review & editing. Mattias Hedenström: Formal analysis, Writing – review & editing. Tobias Sparrman: Formal analysis, Writing – review & editing. Mats B. Nilsson: Conceptualization, Methodology, Writing – review & editing, Jürgen Schleucher: Conceptualization, Methodology, Writing – review & editing. Mats Öquist: Conceptualization, Methodology, Funding acquisition, Writing – review & editing, Supervision.

Funding Open access funding provided by Swedish University of Agricultural Sciences. This work was supported by VR, the Swedish Research Council [2017–04369], and FORMAS, a Swedish Research Council for Sustainable Development [2017 – 01006].

Data availability Data will be made available on request.

Declarations

Competing interest The authors declare that they have no known competing financial interests or personal relationships that could have appeared to influence the work reported in this paper.

References

Adler E (1977) Lignin chemistry-past, present and future. Wood Sci Technol 11(3):169–218. https://doi.org/10.1007/BF00365615

Angst G, Mueller KE, Nierop KGJ, Simpson MJ (2021) Plant- or microbial-derived? A review on the molecular composition of stabilized soil organic matter. Soil Biol Biochem 156:108189. https://doi.org/10.1016/j.soilbio.2021.108189

Bates D, Mächler M, Bolker B, Walker S (2015) Fitting Linear mixed-effects models using lme4. J Stat Softw 67:1–48. https://doi.org/10.18637/jss.v067.i01

Beillouin D, Corbeels M, Demenois J, Berre D, Boyer A, Fallot A, Feder F, Cardinael R (2023) A global meta-analysis of soil organic carbon in the Anthropocene. Nat Commun 14(1):3700. https://doi.org/10.1038/s41467-023-39338-z

Berg B, Ekbohm G (1991) Litter mass-loss rates and decomposition patterns in some needle and leaf litter types. Long-term decomposition in a scots pine forest. VII. Can J Bot 69(7):1449–1456. https://doi.org/10.1139/b91-187

Berg B, McClaugherty C (2020) Plant Litter: decomposition, humus formation, carbon sequestration. Springer International Publishing, Cham

Berg B, Ekbohm G, McClaugherty C (1984) Lignin and holocellulose relations during long-term decomposition of some forest litters. Long-term decomposition in a scots pine forest. IV. Can J Bot 62(12):2540–2550. https://doi.org/10.1139/b84-345

Bertrand I, Chabbert B, Kurek B, Recous S (2006) Can the biochemical features and histology of wheat residues explain their decomposition in Soil? Plant Soil 281(1–2):291–307. https://doi.org/10.1007/s11104-005-4628-7

Boerjan W, Ralph J, Baucher M (2003) Lignin biosynthesis. Annu Rev Plant Biol 54(1):519–546. https://doi.org/10.1146/annurev.arplant.54.031902.134938

Bonner MT, Castro D, Schneider AN, Sundström G, Hurry V, Street NR, Näsholm T (2019) Why does nitrogen addition to forest soils inhibit decomposition? Soil Biol Biochem 137(March):107570. https://doi.org/10.1016/j.soilbio.2019.107570

Brown ME, Chang MC (2014) Exploring bacterial lignin degradation. Curr Opin Chem Biol 19:1–7. https://doi.org/10.1016/j.cbpa.2013.11.015

Cadisch G, Giller KE, Giller KE (1997) Driven by nature. CAB International, Wallingford, Plant Litter Quality and Decomposition, p 432

Campo J, Stijsiger RJ, Nadal-Romero E, Cammeraat ELH (2019) The effects of land abandonment and long-term afforestation practices on the organic carbon stock and lignin content of Mediterranean humid mountain soils. Eur J Soil Sci 70(5):947–959. https://doi.org/10.1111/ejss.12799

Chen X, Ouyang X, Li J, Zhao Y-L (2021) Natural syringyl mediators accelerate laccase-catalyzed β-O-4 cleavage and Cα-Oxidation of a Guaiacyl Model substrate via an aggregation mechanism. ACS Omega 6(35):22578–22588. https://doi.org/10.1021/acsomega.1c02501

Cotrufo MF, Wallenstein MD, Boot CM, Denef K, Paul E (2013) The Microbial Efficiency-Matrix stabilization (MEMS) framework integrates plant litter decomposition with soil organic matter stabilization: do labile plant inputs form stable soil organic matter? Glob Change Biol 19(4):988–995. https://doi.org/10.1111/gcb.12113

Cotrufo MF, Soong JL, Horton AJ, Campbell EE, Haddix ML, Wall DH, Parton WJ (2015) Formation of soil organic matter via biochemical and physical pathways of litter mass loss. Nat Geosci 8(10):776–779. https://doi.org/10.1038/ngeo2520

Datta R, Kelkar A, Baraniya D, Molaei A, Moulick A, Meena RS, Formanek P (2017) Enzymatic degradation of lignin in soil: a review. Sustain (Switzerland) 9(7). https://doi.org/10.3390/su9071163

de Boer W, Folman LB, Summerbell RC, Boddy L (2005) Living in a fungal world: impact of fungi on soil bacterial niche development★. FEMS Microbiol Rev 29(4):795–811. https://doi.org/10.1016/j.femsre.2004.11.005

Del Río JC, Rencoret J, Prinsen P, Martínez ÁT, Ralph J, Gutiérrez A (2012) Structural characterization of wheat straw lignin as revealed by analytical pyrolysis, 2D-NMR, and reductive cleavage methods. J Agric Food Chem 60(23):5922–5935. https://doi.org/10.1021/jf301002n

Escamez S, Robinson KM, Luomaranta M, Gandla ML, Mähler N, Yassin Z, Grahn T, Scheepers G, Stener L-G, Jansson S, Jönsson LJ, Street NR, Tuominen H (2023) Genetic markers and tree properties predicting wood biorefining potential in aspen (Populus tremula) bioenergy feedstock. Biotechnol Biofuels Bioprod 16(1):65. https://doi.org/10.1186/s13068-023-02315-1

Friedlingstein P, O'Sullivan M, Jones MW, Andrew RM, Hauck J, Olsen A, Peters GP, Peters W, Pongratz J, Sitch S, Le Quéré C, Canadell JG, Ciais P, Jackson RB, Alin S, Aragão LEOC, Arneth A, Arora V, Bates NR, Becker M, Benoit-Cattin A, Bittig HC, Bopp L, Bultan S, Chandra N, Chevallier F, Chini LP, Evans W, Florentie L, Forster PM, Gasser T, Gehlen M, Gilfillan D, Gkritzalis T, Gregor L, Gruber N, Harris I, Hartung K, Haverd V, Houghton RA, Ilyina T, Jain AK, Joetzjer E, Kadono K, Kato E, Kitidis V, Korsbakken JI, Landschützer P, Lefèvre N, Lenton A, Lienert S, Liu Z, Lombardozzi D, Marland G, Metzl N, Munro DR, Nabel JEMS, Nakaoka S-I, Niwa Y, O'Brien K, Ono T, Palmer PI, Pierrot D, Poulter B, Resplandy L, Robertson E, Rödenbeck C, Schwinger J, Séférian R, Skjelvan I, Smith AJP, Sutton AJ, Tanhua T, Tans PP, Tian H, Tilbrook B, van der Werf G, Vuichard N, Walker AP, Wanninkhof R, Watson AJ, Willis D, Wiltshire AJ, Yuan W, Yue X, Zaehle S (2020) Global Carbon Budget 2020. Earth Syst Sci Data 12(4):3269–3340. https://doi.org/10.5194/essd-12-3269-2020

Gerber L, Eliasson M, Trygg J, Moritz T, Sundberg B (2012) Multivariate curve resolution provides a high-throughput data processing pipeline for pyrolysis-gas chromatography/mass spectrometry. J Anal Appl Pyrol 95:95–100. https://doi.org/10.1016/j.jaap.2012.01.011

Girden ER (1992) ANOVA: repeated measures. Sage, Newbury Park, CA. https://doi.org/10.4135/9781412983419

Goacher RE, Mottiar Y, Mansfield SD (2021) ToF-SIMS imaging reveals that p-hydroxybenzoate groups specifically decorate the lignin of fibres in the xylem of poplar and willow. Holzforschung 75(5):452–462. https://doi.org/10.1515/hf-2020-0130

Goñi MA, Nelson B, Blanchette RA, Hedges JI (1993) Fungal degradation of wood lignins: geochemical perspectives from CuO-derived phenolic dimers and monomers. Geochim Cosmochim Acta 57(16):3985–4002. https://doi.org/10.1016/0016-7037(93)90348-Z

He M, Zhao R, Tian Q, Huang L, Wang X, Liu F (2019) Predominant effects of litter chemistry on lignin degradation in the early stage of leaf litter decomposition. Plant Soil. https://doi.org/10.1007/s11104-019-04207-6

Herman J, Moorhead D, Berg B (2008) The relationship between rates of lignin and cellulose decay in aboveground forest litter. Soil Biol Biochem 40(10):2620–2626. https://doi.org/10.1016/j.soilbio.2008.07.003

Huang W, Hammel KE, Hao J, Thompson A, Timokhin VI, Hall SJ (2019) Enrichment of Lignin-derived carbon in mineral-associated soil organic matter. Environ Sci Technol 53(13):7522–7531. https://doi.org/10.1021/acs.est.9b01834

Huang W, Yu W, Yi B, Raman E, Yang J, Hammel KE, Timokhin VI, Lu C, Howe A, Weintraub-Leff SR, Hall SJ (2023) Contrasting geochemical and fungal controls on decomposition of lignin and soil carbon at continental scale. Nat Commun 14(1):2227. https://doi.org/10.1038/s41467-023-37862-6

Ilstedt U, Nordgren A, Malmer A (2000) Optimum soil water for soil respiration before and after amendment with glucose. Soil Biol Biochem 32(11–12):1591–1599

Jalas J, Suominen J (1989) Atlas Florae Europaeae: volume 3: distribution of vascular plants in Europe. Cambridge University Press, Cambridge

Janusz G, Pawlik A, Sulej J, Świderska-Burek U, Jarosz-Wilkolazka A, Paszczyński A (2017) Lignin degradation: microorganisms, enzymes involved, genomes analysis and evolution. FEMS Microbiol Rev 41(6):941–962. https://doi.org/10.1093/femsre/fux049

Jonsson P, Johansson AI, Gullberg J, Trygg J, Grung AJ, Marklund B, Sjöström S, Antti M, Moritz H (2005) High-Throughput Data Analysis for Detecting and identifying differences between samples in GC/MS-Based metabolomic analyses. Anal Chem 77(17):5635–5642. https://doi.org/10.1021/ac050601e

Jung YS, Lim WT, Park J, Kim Y (2009) Effect of pH on Fenton and Fenton-like oxidation. Environ Technol 30(2):183–190. https://doi.org/10.1080/09593330802468848

Kalbitz K, Kaiser K, Bargholz J, Dardenne P (2006) Lignin degradation controls the production of dissolved organic matter in decomposing foliar litter. Eur J Soil Sci 57(4):504–516. https://doi.org/10.1111/j.1365-2389.2006.00797.x

Karjalainen EJ (1989) The spectrum reconstruction problem. Chemometr Intell Lab Syst 7(1–2):31–38. https://doi.org/10.1016/0169-7439(89)80109-1

Kawai S, Nakagawa M, Ohashi H (2002) Degradation mechanisms of a nonphenolic β-O-4 lignin model dimer by Trametes Versicolor laccase in the presence of 1-hydroxybenzotriazole. Enzym Microb Technol 30(4):482–489. https://doi.org/10.1016/S0141-0229(01)00523-3

Kenward MG, Roger JH (1997) Small sample inference for fixed effects from Restricted Maximum Likelihood. Biometrics 53(3):983–997. https://doi.org/10.2307/2533558

Kim H, Ralph J (2010) Solution-state 2D NMR of ball-milled plant cell wall gels in DMSO-d 6/pyridine-d5. Org Biomol Chem 8(3):576–591. https://doi.org/10.1039/b916070a

Kim H, Ralph J (2014) A gel-state 2D-NMR method for plant cell wall profiling and analysis: a model study with the amorphous cellulose and xylan from ball-milled cotton linters. Royal Scoiety Chem Adv 4:7549–7560. https://doi.org/10.1039/c3ra46338a

Kim H, Ralph J, Akiyama T (2008) Solution-state 2D NMR of ball-milled Plant Cell Wall gels in DMSO-d 6. Bioenerg Res 1(1):56–66. https://doi.org/10.1007/s12155-008-9004-z

Kirk TK, Tien M, Kersten PJ, Mozuch MD, Kalyanaraman B (1986) Ligninase of Phanerochaete chrysosporium. Mechanism of its degradation of the non-phenolic arylglycerol beta-aryl ether substructure of lignin. Biochem J 236(1):279–287. https://doi.org/10.1042/bj2360279

Klotzbücher T, Kaiser K, Guggenberger G, Gatzek C, Kalbitz K (2011) A new conceptual model for the fate of lignin in decomposing plant litter. Ecology 92(5):1052–1062. https://doi.org/10.1890/10-1307.1

Kuznetsova A, Brockhoff PB, Christensen RHB (2017) lmerTest Package: tests in Linear mixed effects models. J Stat Softw 82:1–26. https://doi.org/10.18637/jss.v082.i13

Lehmann J, Kleber M (2015) The contentious nature of soil organic matter. Nature 528(7580):60–68. https://doi.org/10.1038/nature16069

Liang C, Amelung W, Lehmann J, Kästner M (2019) Quantitative assessment of microbial necromass contribution to soil organic matter. Glob Change Biol 25(11):3578–3590. https://doi.org/10.1111/gcb.14781

Lin Z, Dai Y, Mishra U, Wang G, Shangguan W, Zhang W, Qin Z (2023) Global and regional soil organic carbon estimates: Magnitude and uncertainties. Pedosphere. https://doi.org/10.1016/j.pedsph.2023.06.005

Liu Q, Luo L, Zheng L (2018) Lignins: Biosynthesis and Biological functions in plants. Int J Mol Sci 19(2):335. https://doi.org/10.3390/ijms19020335

Lourenço A, Pereira H (2018) Compositional Variability of Lignin in Biomass. In: Poletto M (ed) Lignin - Trends and Applications. InTech

Luquez V, Hall D, Albrectsen BR, Karlsson J, Ingvarsson P, Jansson S (2008) Natural phenological variation in aspen (Populus tremula): the SwAsp collection. Tree Genet Genomes 4(2):279–292. https://doi.org/10.1007/s11295-007-0108-y

Lv J, Huang Z, Luo L, Zhang S, Wang Y (2022) Advances in Molecular and Microscale characterization of Soil Organic Matter: current limitations and Future prospects. Environ Sci Technol 56(18):12793–12810. https://doi.org/10.1021/acs.est.2c00421

Machinet GE, Bertrand I, Chabbert B, Recous S (2009) Decomposition in soil and chemical changes of maize roots with genetic variations affecting cell wall quality. Eur J Soil Sci 60(2):176–185. https://doi.org/10.1111/j.1365-2389.2008.01109.x

Mao J, Cao X, Olk DC, Chu W, Schmidt-Rohr K (2017) Advanced solid-state NMR spectroscopy of natural organic matter. Progress Nucl Magn Reson Spectrosc 100:17–51. https://doi.org/10.1016/j.pnmrs.2016.11.003

Miltner A, Zech W (1998) Beech leaf litter lignin degradation and transformation as influenced by mineral phases. Org Geochem 28(7):457–463. https://doi.org/10.1016/S0146-6380(98)00019-9

Moorhead DL, Sinsabaugh RL (2006) A theoretical model of Litter Decay and Microbial Interaction. Ecol Monogr 76(2):151–174. https://doi.org/10.1890/0012-9615(2006)076[0151:ATMOLD]2.0.CO;2

Moura JCMS, Bonine CAV, De Oliveira Fernandes Viana J, Dornelas MC, Mazzafera P (2010) Abiotic and biotic stresses and changes in the Lignin content and composition in plants. J Integr Plant Biol 52(4):360–376. https://doi.org/10.1111/j.1744-7909.2010.00892.x

Nordgren A (1988) Apparatus for the continuous, long-term monitoring of soil respiration rate in large numbers of samples. Soil Biol Biochem 20(6):955–957. https://doi.org/10.1016/0038-0717(88)90110-1

Nordgren A (1992) A method for determining microbially available N and P in an organic soil. Biol Fertil Soils 13(4):195–199. https://doi.org/10.1007/BF00340575

Nordgren A, Bååth E, Söderström B (1988) Evaluation of soil respiration characteristics to assess heavy metal effects on soil microorganisms using glutamic acid as a substrate. Soil Biol Biochem 20(6):949–954. https://doi.org/10.1016/0038-0717(88)90109-5

Ong HC, Chen W-H, Singh Y, Gan YY, Chen C-Y, Show PL (2020) A state-of-the-art review on thermochemical conversion of biomass for biofuel production: a TG-FTIR approach. Energy Conv Manag 209:112634. https://doi.org/10.1016/j.enconman.2020.112634

Op De Beeck M, Troein C, Peterson C, Persson P, Tunlid A (2018) Fenton reaction facilitates organic nitrogen acquisition by an ectomycorrhizal fungus. New Phytol 218(1):335–343. https://doi.org/10.1111/nph.14971

Otto A, Simpson MJ (2006) Evaluation of CuO oxidation parameters for determining the source and stage of lignin degradation in soil. Biogeochemistry 80(2):121–142. https://doi.org/10.1007/s10533-006-9014-x

Pisani O, Frey SD, Simpson AJ, Simpson MJ (2015) Soil warming and nitrogen deposition alter soil organic matter composition at the molecular-level. Biogeochemistry 123(3):391–409. https://doi.org/10.1007/s10533-015-0073-8

Polman EMN, Gruter G-JM, Parsons JR, Tietema A (2021) Comparison of the aerobic biodegradation of biopolymers and the corresponding bioplastics: a review. Sci Total Environ 753:141953. https://doi.org/10.1016/j.scitotenv.2020.141953

Prescott CE (2010) Litter decomposition: what controls it and how can we alter it to sequester more carbon in forest soils? Biogeochemistry 101(1):133–149. https://doi.org/10.1007/s10533-010-9439-0

R Core Team (2021) R: a language and environment for statistical computing. R Foundation for Statistical Computing, Vienna, Austria

Ralph J, Lundquist K, Brunow G, Lu F, Kim H, Schatz PF, Marita JM, Hatfield RD, Ralph SA, Christensen JH, Boerjan W (2004) Lignins: natural polymers from oxidative coupling of 4-hydroxyphenyl- propanoids. Phytochem Rev 3(1–2):29–60. https://doi.org/10.1023/B:PHYT.0000047809.65444.a4

Renström A, Choudhary S, Gandla ML, Jönsson LJ, Hedenström M, Jämtgård S, Tuominen H (2024) The effect of nitrogen source and levels on hybrid aspen tree physiology and wood formation. Physiol Plant 176(1):e14219. https://doi.org/10.1111/ppl.14219

Saiya-Cork KR, Sinsabaugh RL, Zak DR (2002) The effects of long term nitrogen deposition on extracellular enzyme activity in an Acer saccharum forest soil. Soil Biol Biochem 34(9):1309–1315. https://doi.org/10.1016/S0038-0717(02)00074-3

Schimel JP, Weintraub MN (2003) The implications of exoenzyme activity on microbial carbon and nitrogen limitation in soil: a theoretical model. Soil Biol Biochem 35(4):549–563. https://doi.org/10.1016/S0038-0717(03)00015-4

Searle SR, Speed FM, Milliken GA (1980) Population marginal means in the Linear Model: an alternative to least squares means. Am Stat 34(4):216–221. https://doi.org/10.1080/00031305.1980.10483031

Shah F, Schwenk D, Nicolás C, Persson P, Hoffmeister D, Tunlid A (2015) Involutin is an fe 3 + reductant secreted by the Ectomycorrhizal Fungus Paxillus involutus during Fenton-based decomposition of Organic Matter. Appl Environ Microbiol 81(24):8427–8433. https://doi.org/10.1128/aem.02312-15

Sinsabaugh RL (2010) Phenol oxidase, peroxidase and organic matter dynamics of soil. Soil Biol Biochem 42(3):391–404. https://doi.org/10.1016/j.soilbio.2009.10.014

Smith DCC (1955) p-Hydroxybenzoate groups in the lignin of aspen (populus tremula). J Chem Soc 2347. https://doi.org/10.1039/jr9550002347

Soucémarianadin LN, Erhagen B, Nilsson MB, Öquist MG, Immerzeel P, Schleucher J (2017) Two dimensional NMR spectroscopy for molecular characterization of soil organic matter: application to boreal soils and litter. Org Geochem J 113:184–195. https://doi.org/10.1016/j.orggeochem.2017.06.019

Stockmann U, Adams MA, Crawford JW, Field DJ, Henakaarchchi N, Jenkins M, Minasny B, McBratney AB, Courcelles V, de Singh R, Wheeler K, Abbott I, Angers L, Baldock DA, Bird J, Brookes M, Chenu PC, Jastrow C, Lal JD, Lehmann R, O'Donnell J, Parton AG, Whitehead WJ, Zimmermann D (2013) The knowns, known unknowns and unknowns of sequestration of soil organic carbon. Agric Ecosyst Environ 164:80–99. https://doi.org/10.1016/j.agee.2012.10.001

Strukelj M, Brais S, Quideau SA, Oh S-W (2012) Chemical transformations of deadwood and foliar litter of mixed boreal species during decomposition. Can J Res 42(4):772–788. https://doi.org/10.1139/x2012-027

Talbot JM, Yelle DJ, Nowick J, Treseder KK (2012) Litter decay rates are determined by lignin chemistry. Biogeochemistry 108(1–3):279–295. https://doi.org/10.1007/s10533-011-9599-6

Thevenot M, Dignac M-F, Rumpel C (2010) Fate of lignins in soils: a review. Soil Biol Biochem 42(8):1200–1211. https://doi.org/10.1016/j.soilbio.2010.03.017

Tolu J, Gerber L, Boily J-F, Bindler R (2015) High-throughput characterization of sediment organic matter by pyrolysis–gas chromatography/mass spectrometry and multivariate curve resolution: a promising analytical tool in (paleo)limnology. Anal Chim Acta 880:93–102. https://doi.org/10.1016/j.aca.2015.03.043

Van Erven G, Hilgers R, Waard PD, Gladbeek E-J, Van Berkel WJH, Kabel MA (2019) Elucidation of in situ ligninolysis mechanisms of the selective White-Rot Fungus *Ceriporiopsis subvermispora*. ACS Sustainable Chem Eng 7(19):16757–16764. https://doi.org/10.1021/acssuschemeng.9b04235

vandenEnden L, Frey SD, Nadelhoffer KJ, LeMoine JM, Lajtha K, Simpson MJ (2018) Molecular-level changes in soil organic matter composition after 10 years of litter, root and nitrogen manipulation in a temperate forest. Biogeochemistry 141(2):183–197. https://doi.org/10.1007/s10533-018-0512-4

Vanholme R, Demedts B, Morreel K, Ralph J, Boerjan W (2010) Lignin Biosynthesis and structure. Plant Physiol 153(3):895–905. https://doi.org/10.1104/pp.110.155119

Wardle DA, Nilsson M-C, Zackrisson O, Gallet C (2003) Determinants of litter mixing effects in a Swedish boreal forest. Soil Biol Biochem 35(6):827–835. https://doi.org/10.1016/S0038-0717(03)00118-4

Yue K, Peng C, Yang W, Peng Y, Zhang C, Huang C, Wu F (2016) Degradation of lignin and cellulose during foliar litter decomposition in an alpine forest river. Ecosphere 7(10):e01523. https://doi.org/10.1002/ecs2.1523

Zhu D, Zhang P, Xie C, Zhang W, Sun J, Qian W-J, Yang B (2017) Biodegradation of alkaline lignin by Bacillus ligniniphilus L1. Biotechnol Biofuels 10(1):44. https://doi.org/10.1186/s13068-017-0735-y

Zoghlami A, Paës G (2019) Lignocellulosic biomass: Understanding recalcitrance and predicting hydrolysis. *Frontiers in Chemistry, 7*, 874.

Zuur AF, Ieno EN, Walker N, Saveliev AA, Smith GM (2009) Mixed effects models and extensions in ecology with R. Springer, New York